

Polyelectrolyte-calcium Complexes as a Pre-precursor Induce Biomimetic Mineralization of Collagen

Zihuai Zhou,^{*a} Leiqing Zhang,^{*a} Jiachen Li,^{*b} Ying Shi,^a Zhifang Wu,^{§a} Haiyan Zheng,^a Zhe Wang,^a

Weijia Zhao,^a Haihua Pan,^c Qi Wang,^b Xiaogang Jin,^d Xing Zhang,^e Ruikang Tang^b and Baiping Fu^{#a}

^a The Affiliated Hospital of Stomatology, School of Stomatology, Zhejiang University School of Medicine, and Key Laboratory of Oral Biomedical Research of Zhejiang Province, Hangzhou, Zhejiang, 310006, China

^b Department of Chemistry, Zhejiang University, Hangzhou, Zhejiang, 310027, China

^c Qiushi Academy for Advanced Studies, Zhejiang University, Hangzhou, Zhejiang, 310027, China

^d State Key Lab of CAD & CG, Zhejiang University, Hangzhou, Zhejiang, 310058, China

^e Department of Biophysics, and Center of Cryo-Electron Micrography, Zhejiang University School of Medicine, Hangzhou, Zhejiang, 310058, China

[#] Correspondence and requests for materials should be addressed to Baiping Fu, fbp@zju.edu.cn.

Contents

1. Supporting figures

- (1) The effect of the PAsp and calcium concentrations on the osmolarity of the PAsp-calcium suspensions
- (2) TEM image of the stained reconstituted collagen fibril
- (3) TEM and 3D-STORM images of the collagen fibrils solely treated with the PAsp-Ca suspension for 1 and 2 min
- (4) TEM and HRTEM images with elemental mapping of the collagen fibrils only treated with PAsp-Ca suspension for 3 min
- (5) Surface zeta potentials of the collagen gel
- (6) FTIR spectra of the collagen gels that were treated with the PAsp-Ca suspension, phosphate solution, and incubated for 1 d
- (7) TEM and HRTEM images with elemental mapping of collagen fibrils treated with the PAsp-Ca suspension for 3 min and with the phosphate solution for 1 min
- (8) TEM images of the collagen fibrils treated with the calcium suspension (5.44 M, pH = 9.5) and phosphate solution (3.25 M) sequentially
- (9) TEM and HRTEM images with SAED of the collagen fibrils that were treated with the PAsp-Ca suspension and phosphate solution, each for 3 min, and incubated in deionized water for 1 h
- (10) TEM and HRTEM images with elemental mapping of the collagen fibrils only treated with the phosphate solution for 3 min

- (11) TEM and HRTEM images with element mapping of the collagen fibrils that were treated with the phosphate solution followed by PAsp-Ca suspension, each for 3 min
- (12) Thermogravimetric analysis of mineralized collagen gels mineralized via PCCP and PILP processes.
- (13) TEM images of the collagen fibrils only treated with a concentration gradient of PAsp-Ca suspensions, each 3 min
- (14) XPS spectra for quantification of the calcium in collagen sponges only treated with a concentration gradient of PAsp-Ca suspensions
- (15) Thermogravimetric analysis for quantification of the calcium content in the collagen sponges only treated with a concentration gradient of PAsp-Ca suspensions
- (16) TEM images of the collagen fibrils treated with the PAsp solution, calcium suspension and phosphate solution in sequence
- (17) TEM of the collagen fibrils treated with the PAA-Ca suspension (8 g/L-5.44 M) and phosphate solution (3.25 M)
- (18) The amino acid sequences of collagen fibrils used for molecular dynamics simulation
- (19) The initial structure of collagen in molecular dynamics simulations

2. References

Supporting figures

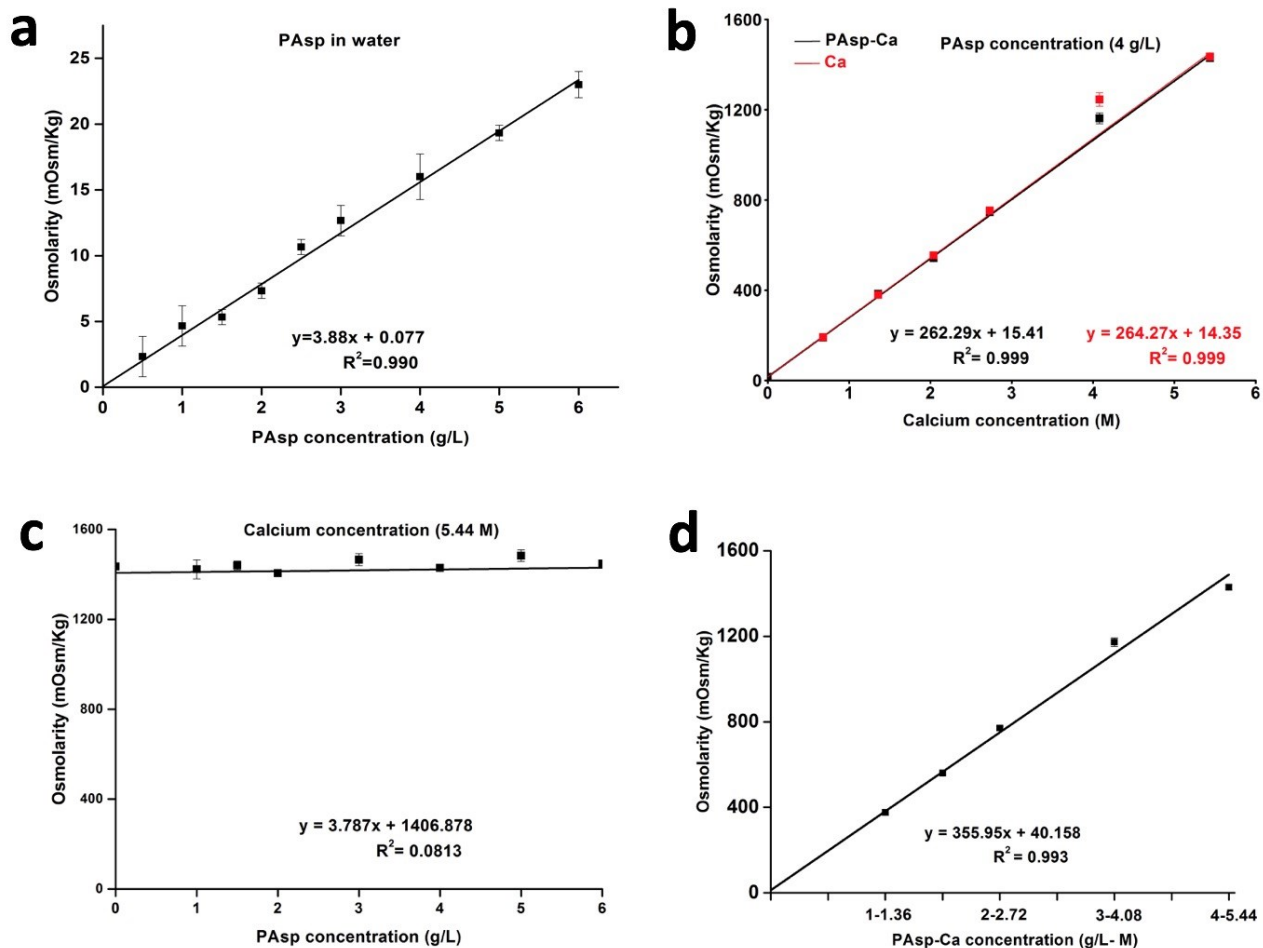


Figure S1. The effect of the PAsp and calcium concentrations on the osmolarity of the PAsp-calcium suspensions. (a) The osmolarity of the pure PAsp solution (0.5 to 6 g/L) increased from 2.33 mOsm/Kg to 23 mOsm/Kg. (b) The osmolarity of the calcium suspensions with and without PAsp as an additive (4 g/L) showed a similar linear increase in osmolarity values. When PAsp was added, the osmolarity slightly decreased due to the formation of PAsp-Ca complexes. (c) PAsp-Ca suspensions with

increasing concentrations of PAsp (from 0 to 6 g/L) demonstrated a negligible influence of PAsp on the osmolarity. (d) The osmolarities of the PAsp-Ca suspensions increased linearly when the concentrations of PAsp and calcium were proportionally increased.

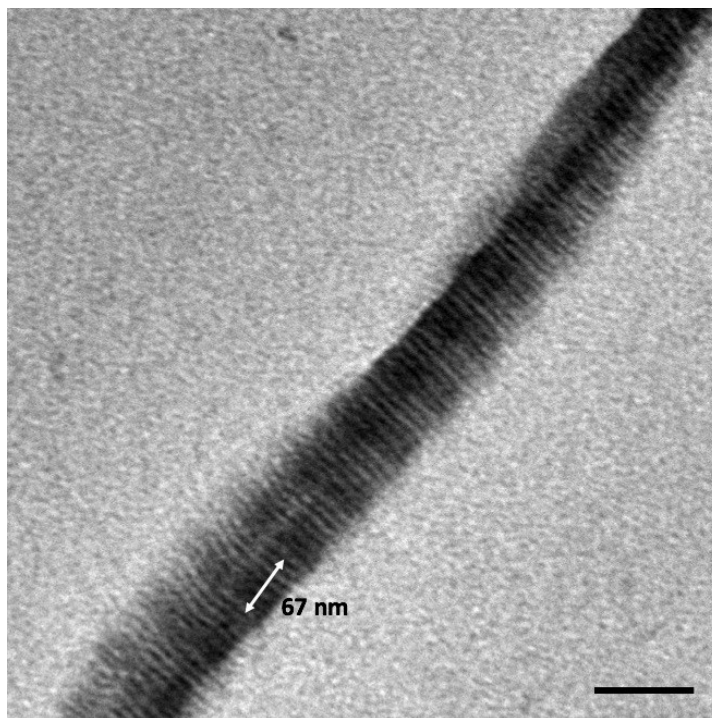


Figure S2. TEM image of the stained reconstituted collagen fibril. The reconstituted collagen fibril coated on TEM Ni grid was stained with uranyl acetate, revealing a typical period of 67 nm of type I collagen. Scale bar: 100 nm.

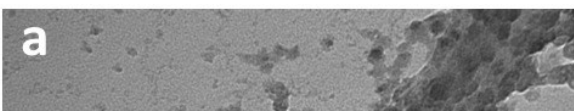


Figure S3. TEM and 3D-STORM images of the collagen fibrils solely treated with the PAsp-Ca suspension for 1 and 2 min. After the unstained collagen fibrils were treated with the FITC-PAsp-Ca (4 g/L-5.44 M) suspension for 1 min (a, c-m) and 2 min (b), a large amount of PAsp-Ca complexes were attracted to the fibrillar surface, and some of them infiltrated into the collagen fibrils. Scale bar: 50 nm (a, b). (c-m) The 3D-STORM images indicating the partial entrance of the FITC-tagged PAsp into the collagen fibril. (c) An immunofluorescently stained collagen fibril is shown in red. (d) The FITC-tagged PAsp-Ca complexes are shown in green. (e) The overlap of “c” and “d” is shown in yellow. Scale bar: 100 nm (c-e). (f-l) The images of z-slices indicating that the PAsp molecules partially entered the intrafibrillar compartments (the yellow areas). The z-slice thickness is 100 nm. Scale bar: 500 nm (f-l). (m) 3-D visualization of the FITC-tagged PAsp-Ca complexes and immunofluorescently labelled collagen fibril.

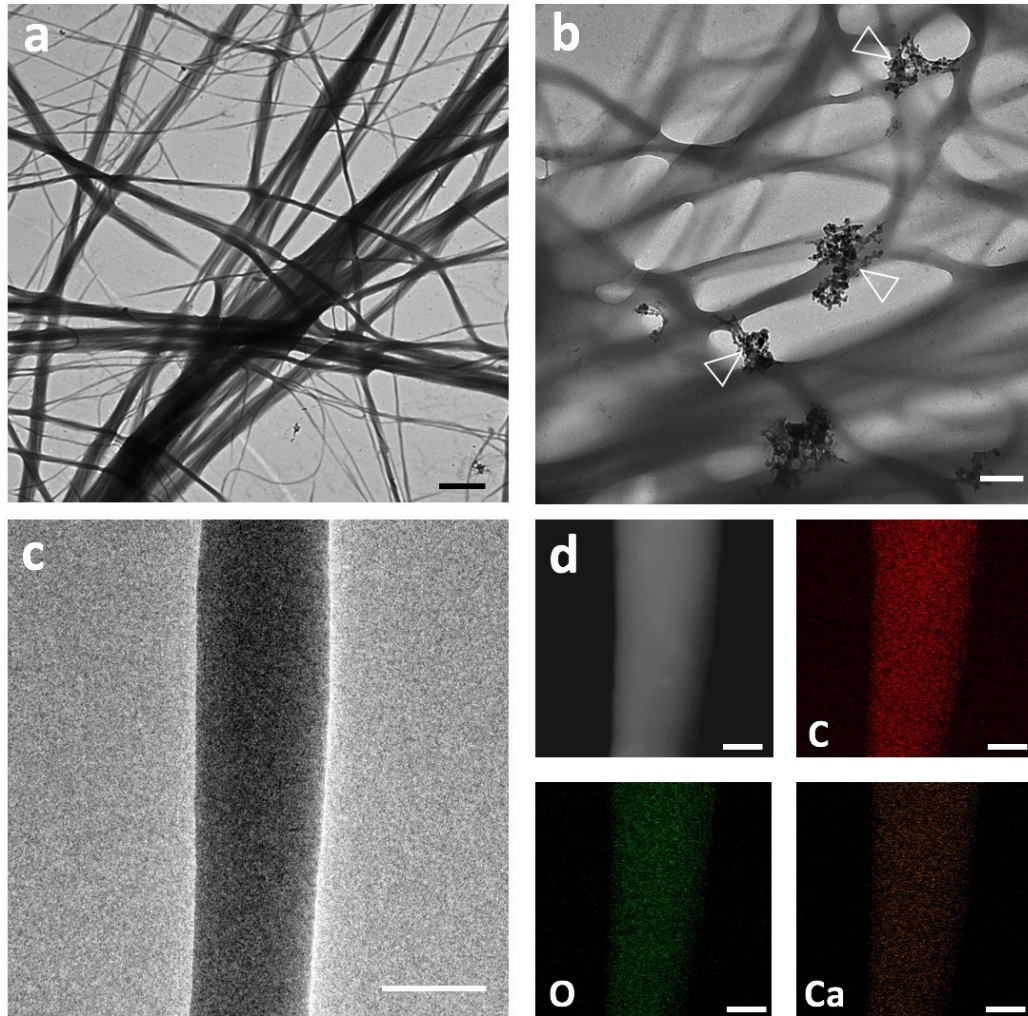


Figure S4. TEM and HRTEM images with elemental mapping of the collagen fibrils only treated with PAsp-Ca suspension for 3 min. (a) After the reconstituted type I collagen fibrils were treated with the PAsp-Ca (4 g/L-5.44 M) suspension for 3 min, the unstained collagen fibrils became much darker in TEM image. Scale bar: 2 μ m. (b) The high-magnification TEM image of “a”. Some PAsp-Ca complexes were observed to attach to the collagen fibrils (arrowhead). Scale bar: 200 nm. (c) The HRTEM image shows high electron density within the collagen fibril. Scale bar: 100 nm. (d) The darkfield image (top left) shows the collagen fibrils full of even electron density. The elemental mappings reveal carbon (red), oxygen (green) and calcium (brown) elements, respectively. Scale bar: 50 nm.

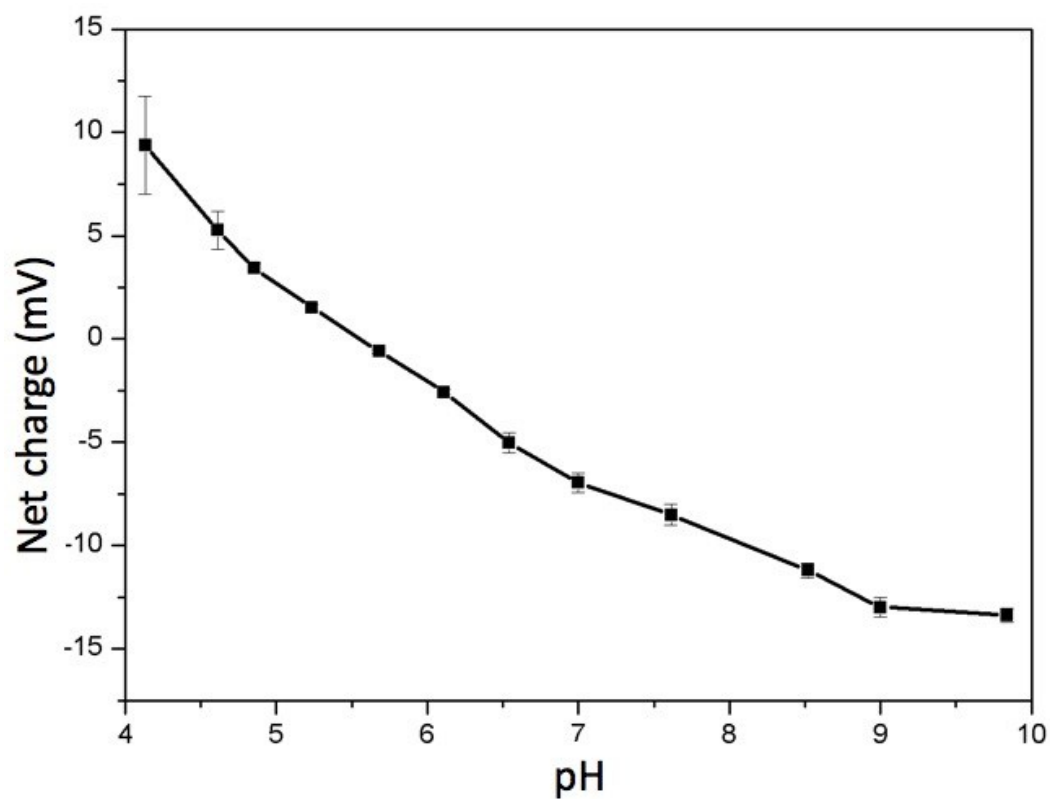


Figure S5. Surface zeta potentials of the collagen gel. The surface zeta potential of collagen decreases to negative charge with an increase of pH value. The decrease of zeta potential decelerates once the pH value reaches up to 9.

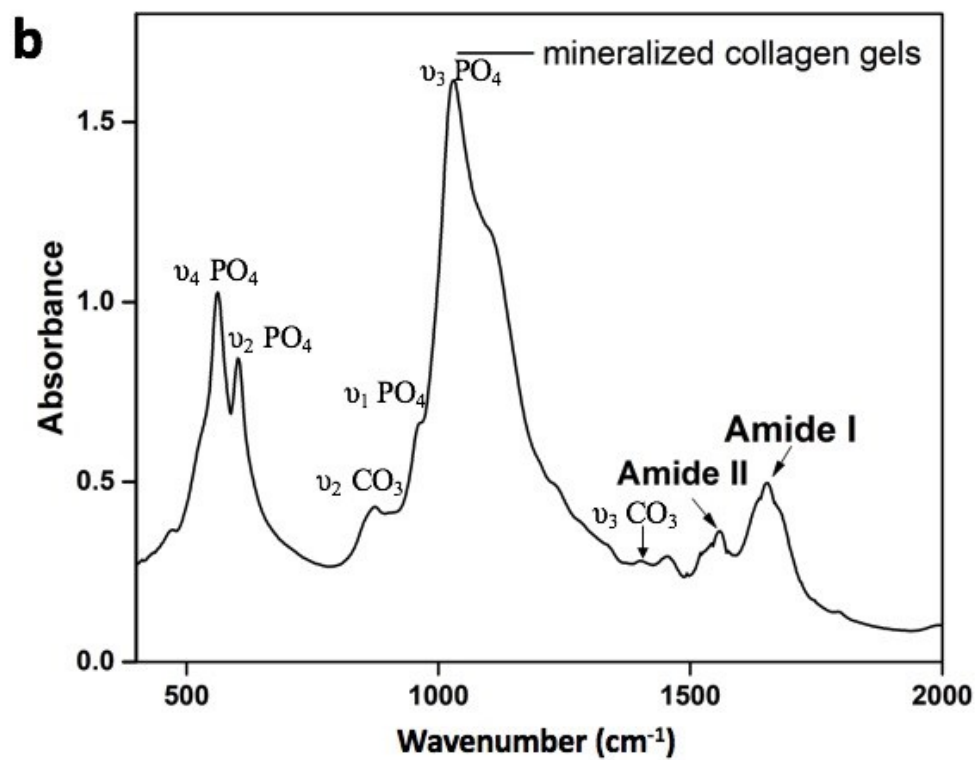
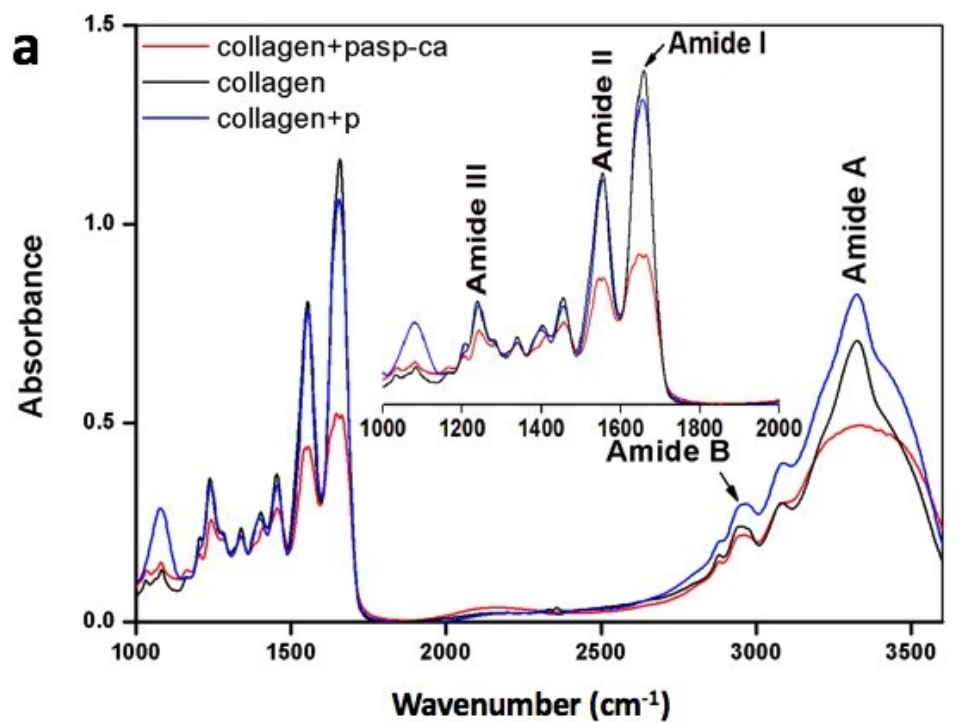


Figure S6. FTIR spectra of the collagen gels that were treated with the PAsp-Ca suspension, phosphate solution, and incubated for 1 d. (a) The FTIR spectra of the reconstituted rat tail collagen gels show

typical amide bands of proteins, in which 1659, 1551, 1238 and 3317 cm^{-1} are ascribed to amide I (C=O stretch), II (NH bend coupled with CN stretch), III (NH bend coupled with CN stretch) and A bands (NH stretch), separately.¹ After the treatment with PAsp-Ca suspension, the peak of amide I band shifted from 1659 cm^{-1} to 1644 cm^{-1} , and the intensities of amide I, II, III and A bands all dropped dramatically. This implies that the calcium ions may enwrap the carboxyl and carbonyl groups and block their vibration. The redshift of the amide I peak indicates that C=O bonds in the collagen are weakened because of the formation of the bonding between the calcium ions and C=O bonds.² The carbonyl oxygen has a nonbonding free electron pair and that might chelate calcium ions with empty electron orbits.² After the treatment with phosphate treatment, no significant change took place except the appearance of the peak at 1082 cm^{-1} , which belonged to $\nu_3 \text{PO}_4$ antisymmetric stretch of phosphate on the collagen fibrils.³ (b) The FTIR spectrum of the mineralized collagen gel confirms that the minerals deposited in collagen gels were carbonated apatite. The peaks at 560 and 601 cm^{-1} are assigned to $\nu_4 \text{PO}_4$ bending modes,⁴ while peaks at 960 and 1032 cm^{-1} are ascribed to $\nu_1 \text{PO}_4$ and $\nu_3 \text{PO}_4$ stretching modes of HAp.⁵ The peaks at 868 and 1404 cm^{-1} are identified as the ν_2 and ν_3 vibrational modes of carbonated apatite.⁶

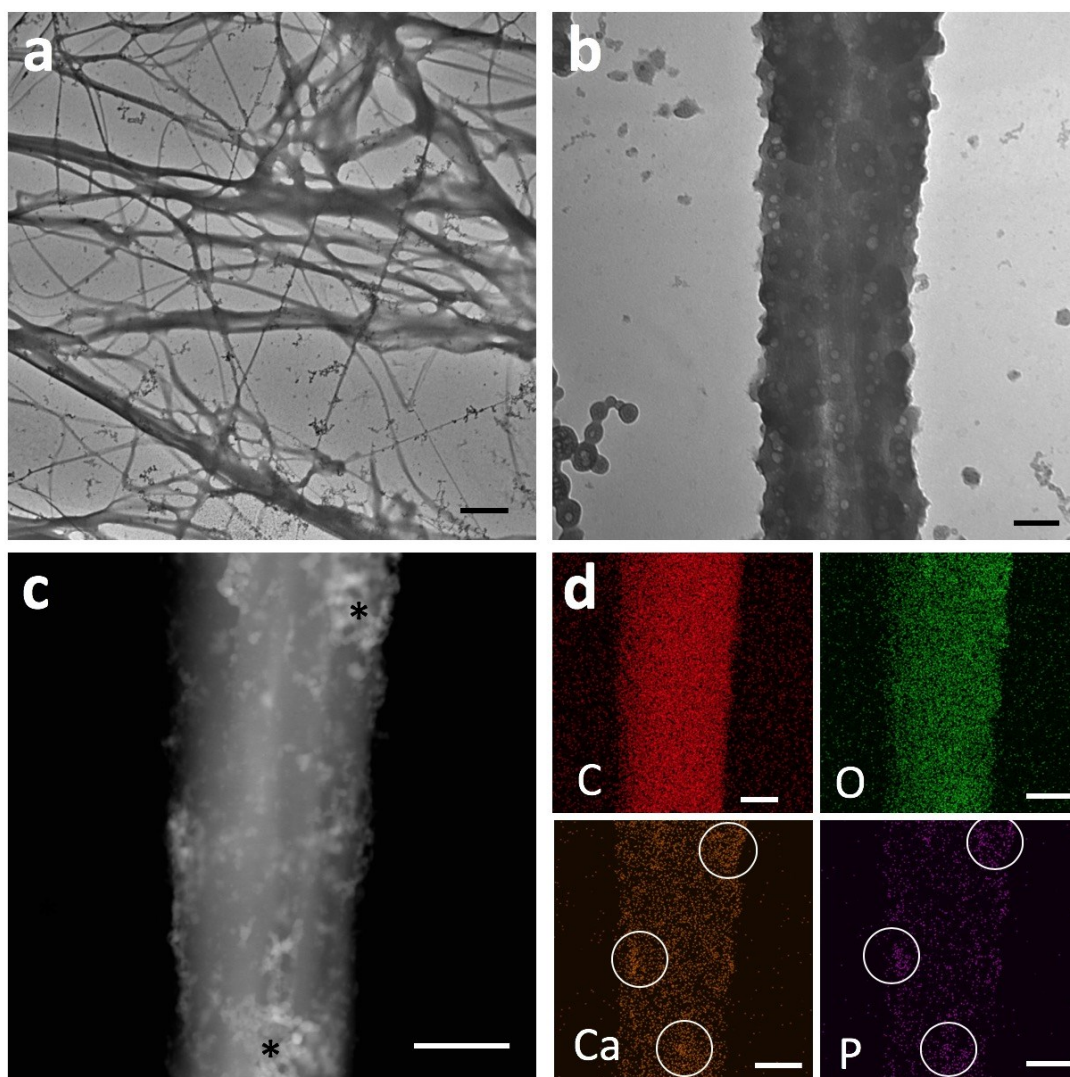


Figure S7. TEM and HRTEM images with elemental mapping of collagen fibrils treated with the PAsp-Ca suspension for 3 min and with the phosphate solution for 1 min. (a) TEM image reveals that the treated collagen fibrils became dark. Scale bar: 1 μm . (b) High magnification of image “a” shows that some beaded substances that seem like ACP crusts are formed on the collagen fibrils. Scale bar: 100 nm. (c) The darkfield image of the collagen fibril reveals that electron distribution is uneven, and some areas are denser (asterisk). Scale bar: 250 nm. (d) The elemental mapping results reveal the even distribution of the carbon and oxygen elements, as well as uneven distribution of the calcium and phosphorus elements. The distributions of the latter two elements (Ca, P) are fully consistent in the regional variations during the incipient aggregations, in which the circles indicate the comparatively

concentrated calcium and phosphorus. Scale bar: 100 nm. Carbon: red, oxygen: green, calcium: brown, and phosphorus: purple.

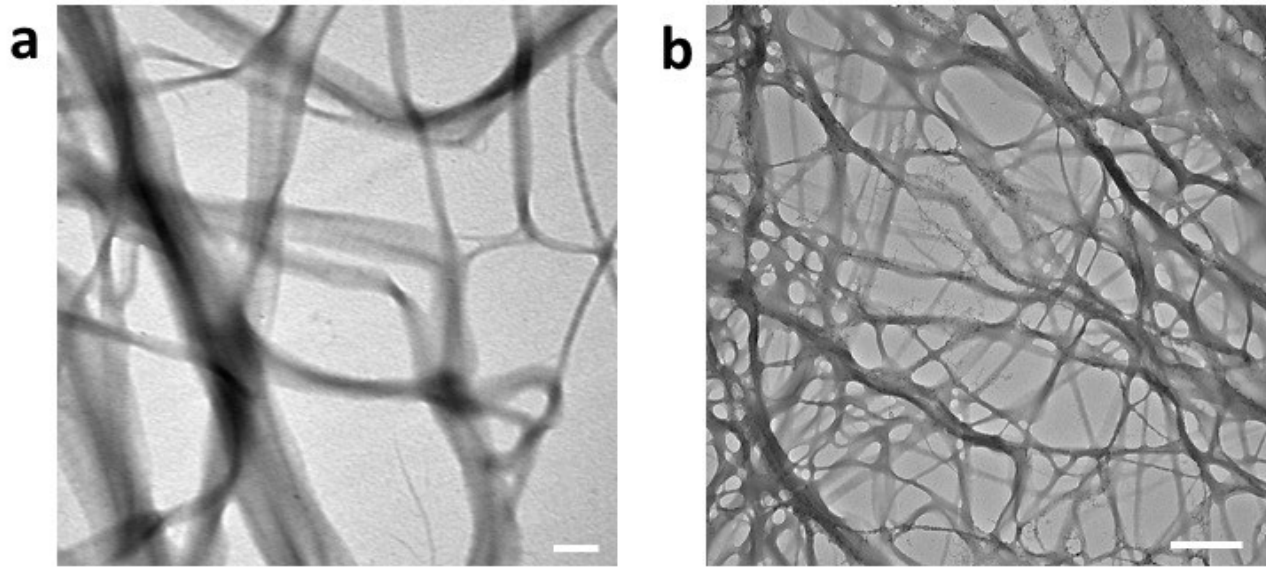


Figure S8. TEM images of the collagen fibrils treated with the calcium suspension (5.44 M, pH = 9.5) and phosphate solution (3.25 M) sequentially. (a) After the collagen fibrils were treated with the calcium chloride suspension and phosphate solution, each 3 min, they were not mineralized. Scale bar: 200 nm. (b) TEM image of the collagen fibrils that were further incubated in artificial saliva for 1 h shows that collagen fibrils were still not mineralized and some extrafibrillar minerals were generated. Scale bar: 500 nm.

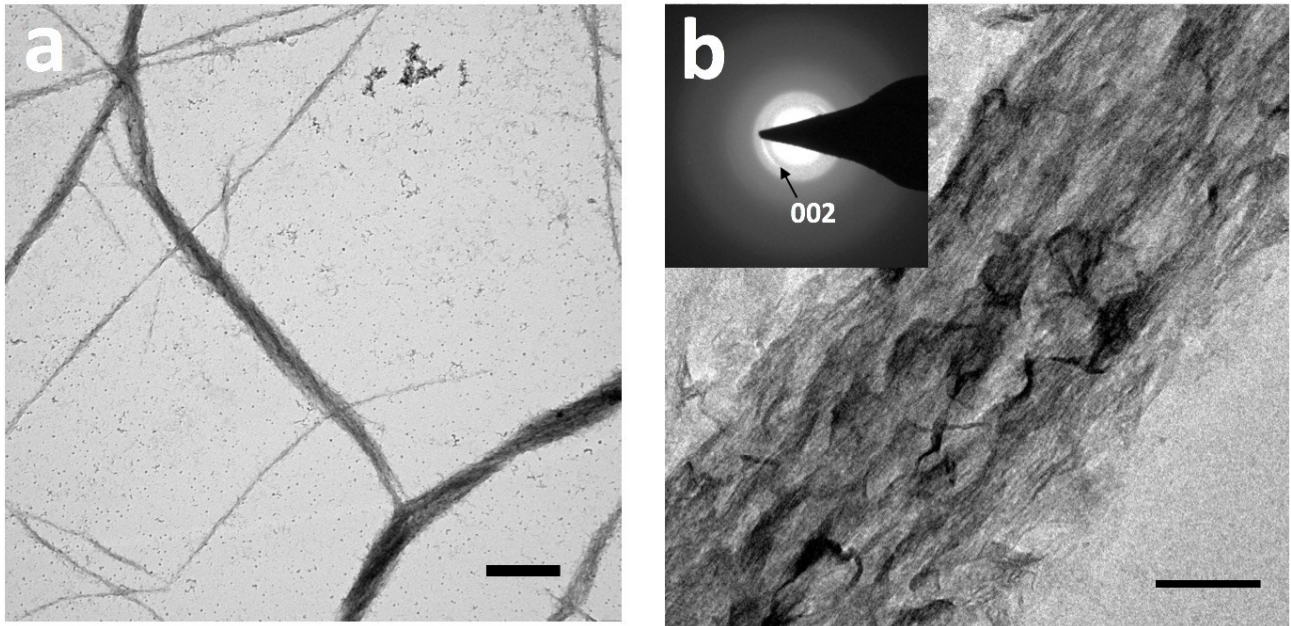


Figure S9. TEM and HRTEM images with SAED of the collagen fibrils that were treated with the PAsp-Ca suspension and phosphate solution, each for 3 min, and incubated in deionized water for 1 h. (a) TEM image reveals the electron-dense collagen fibrils. Scale bar: 200 nm. (b) HRTEM image with SAED pattern demonstrates the distinct (002) plane of crystallites within fibrils and the c-axis parallel to the long-axis of collagen. Scale bar: 100 nm.

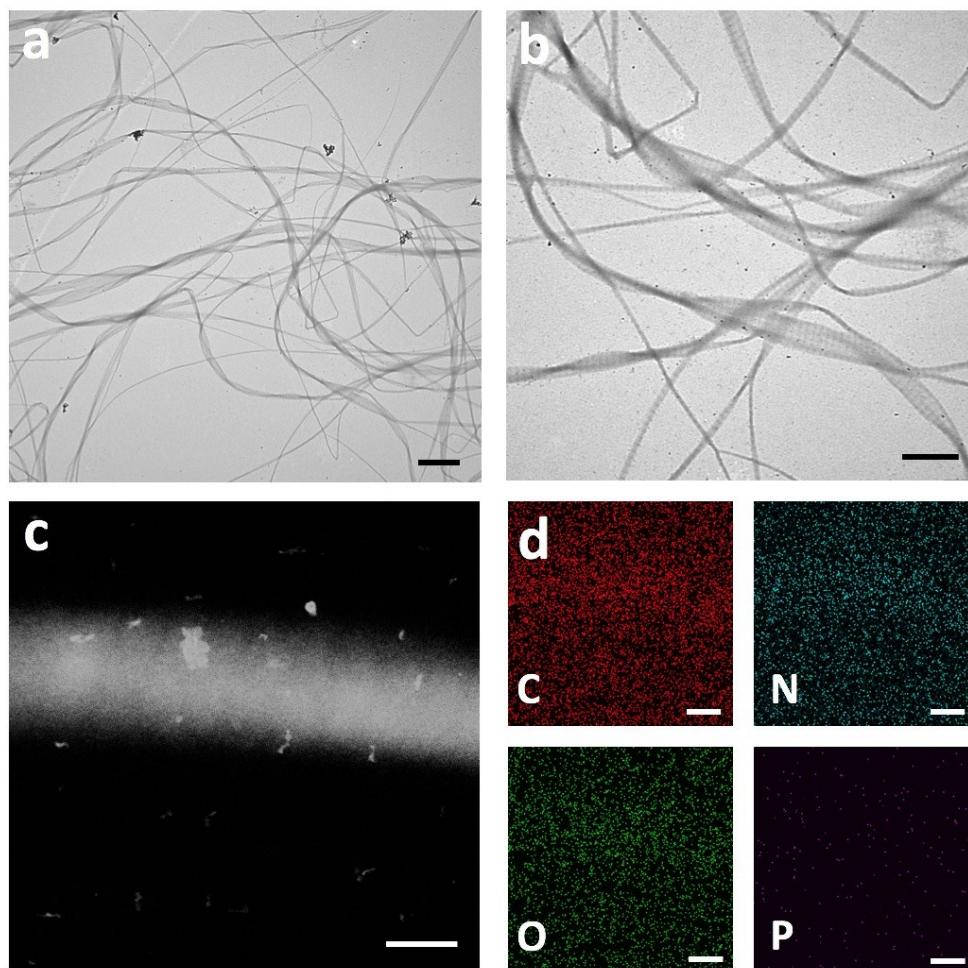


Figure S10. TEM and HRTEM images with elemental mapping of the collagen fibrils only treated with the phosphate solution for 3 min. (a) TEM image reveals a low electron density of the collagen fibrils. Scale bar: 1 μm . (b) High magnification of “a” shows typical periodic banding structures of the collagen fibrils. Scale bar: 500 nm. (c) The darkfield image of the collagen fibril shows an obscure conformation with alternating light and dark bands. Scale bar: 100 nm. (d) The elemental mapping reveals the even distribution of the elements carbon (red), nitrogen (blue), and oxygen (green) on the collagen fibrils, as well as the scarce distribution of phosphorus (purple). Scale bar: 100 nm.

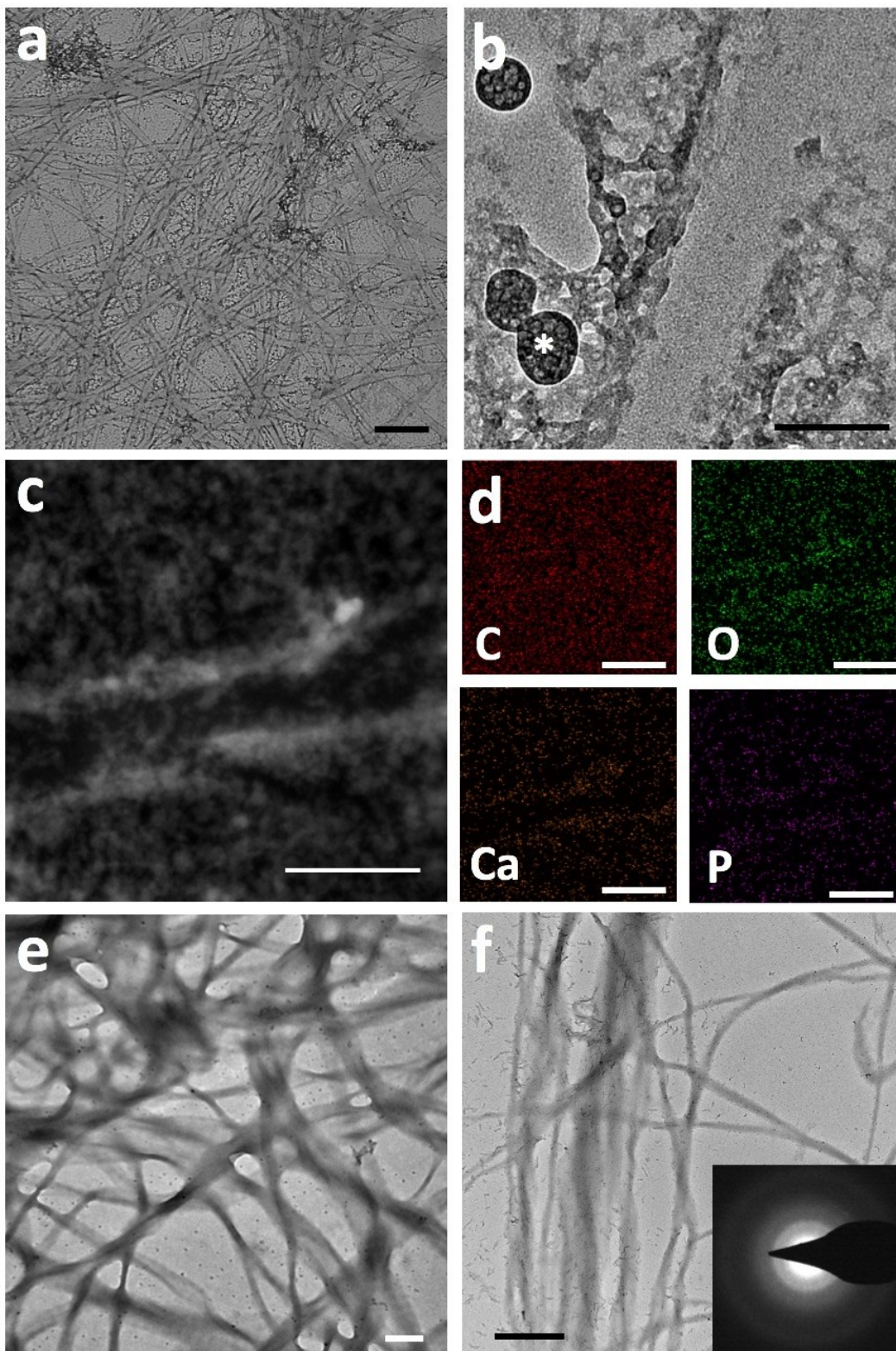


Figure S11. TEM and HRTEM images with element mapping of the collagen fibrils that were treated with the phosphate solution followed by PAsp-Ca suspension, each for 3 min. (a) HRTEM image

reveals that the electron density is extremely low in the collagen fibrils and a large amount of amorphous calcium phosphate is intercepted outside the collagen fibrils. Scale bar: 500 nm. (b) High-magnification HRTEM image of “a” shows spherical ACP nanoparticles outside the collagen fibril (asterisk). The banding structure of fibril is obscured because of few intrafibrillar mineral. Scale bar: 100 nm. (c) The darkfield image reveals that amorphous particles are distributed outside of the collagen fibrils. Scale bar: 100 nm. (d) The element mapping shows that the carbon (red) is evenly distributed, but calcium (brown) and phosphorus (purple) are distributed outside of the collagen fibril. Scale bar: 100 nm. After the pretreated collagen fibrils were incubated in the artificial saliva for 30 min (e, scale bar: 200 nm) and 1 h (f, scale bar: 500 nm), few intrafibrillar mineral could be identified within collagen fibrils (e, f) without crystalline arc (f, inset).

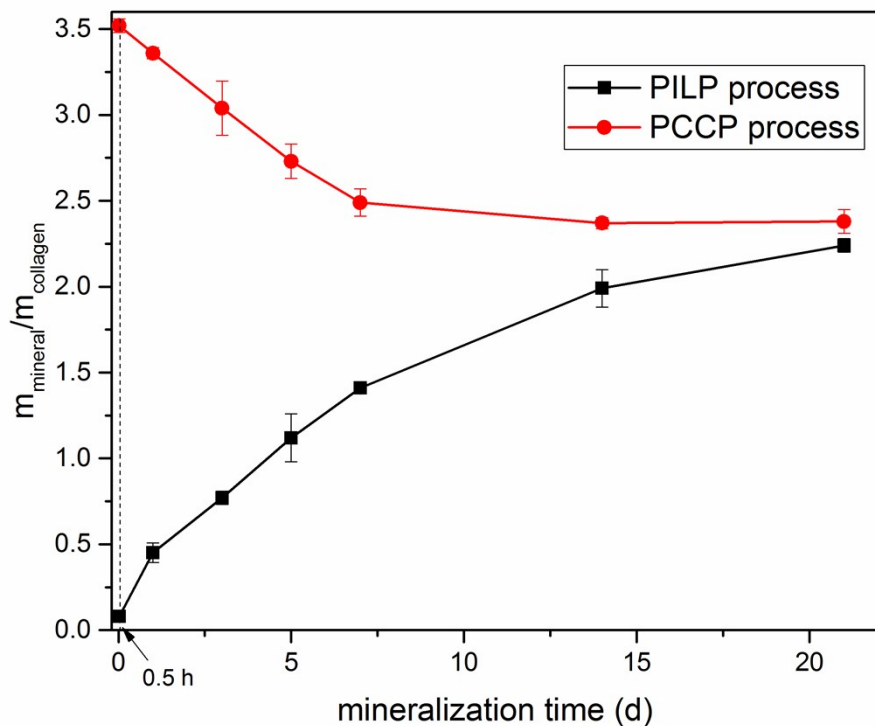


Figure S12. Thermogravimetric analysis of mineralized collagen gels mineralized via PCCP and PILP processes. The PCCP process provided sufficient calcium and phosphate sources for mineralization of collagen gels with a mineral/organics ratio of 3.52 at the beginning. The mineral content of the gel gradually decreased to approximately 2.37 in a constant state after 14 days of incubation. In contrast, the mineral content in the gel mineralized via PILP process gradually increased over time (from 0.08 at 0.5 h to 2.24 at 21 d). There is no significant difference of the mineral contents between PILP and PCCP process at 21 days.

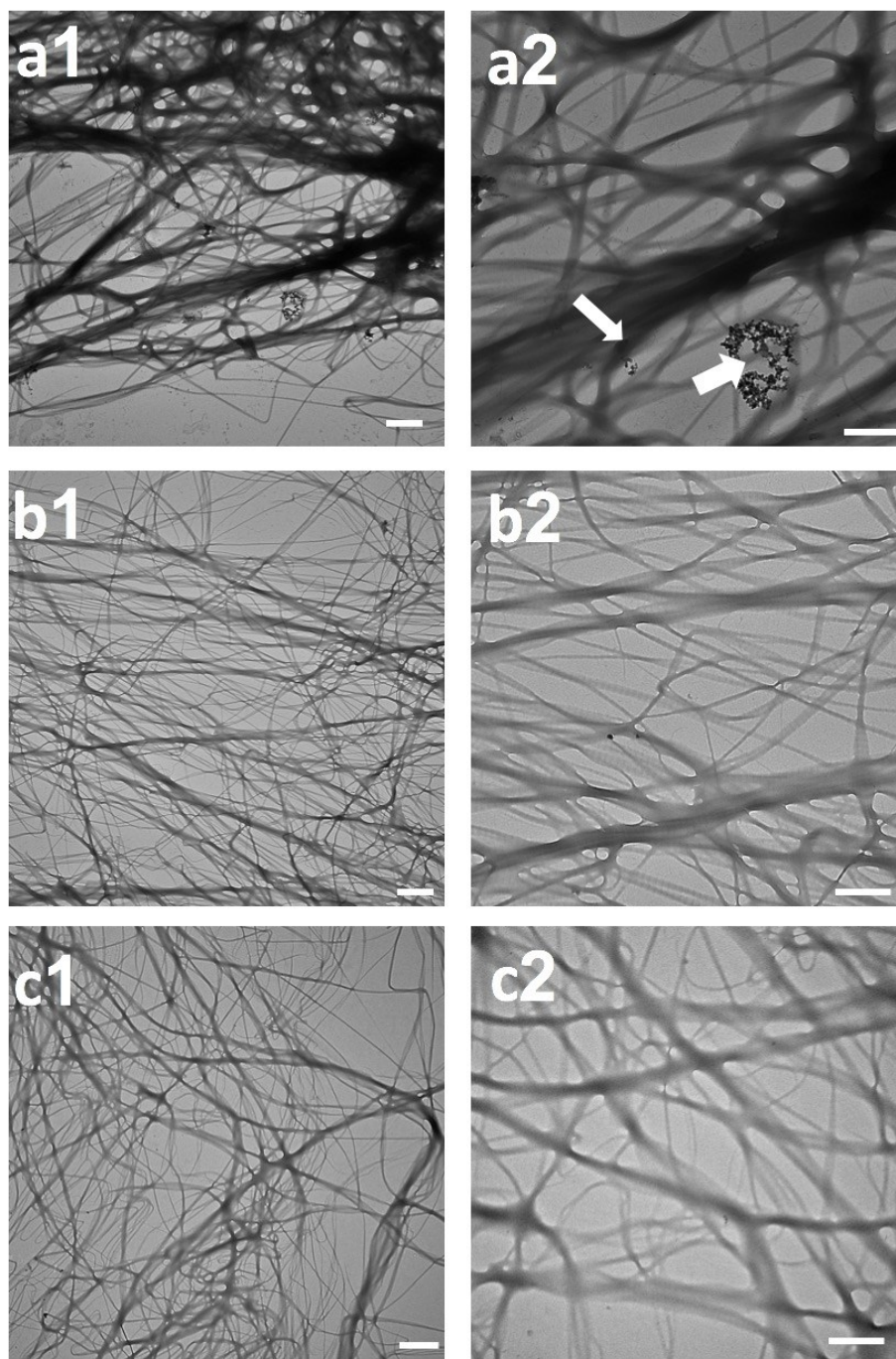


Figure S13. TEM images of the collagen fibrils only treated with a concentration gradient of PAsp-Ca suspensions, each 3 min. PAsp-Ca concentration: (a) 4 g/L-5.44 M, (b) 2 g/L-2.72 M, (c) 1 g/L-1.36 M, left images (a1, b1, c1) are low magnification (scale bar: 1 μ m) of right images (a2, b2, c2) (scale bar: 500 nm). The electron densities of the collagen fibrils in “b” and “c” are strikingly lighter than that in “a”. There is a few visible PAsp-Ca complexes (arrow) detected in “a” but none in “b” and “c”.

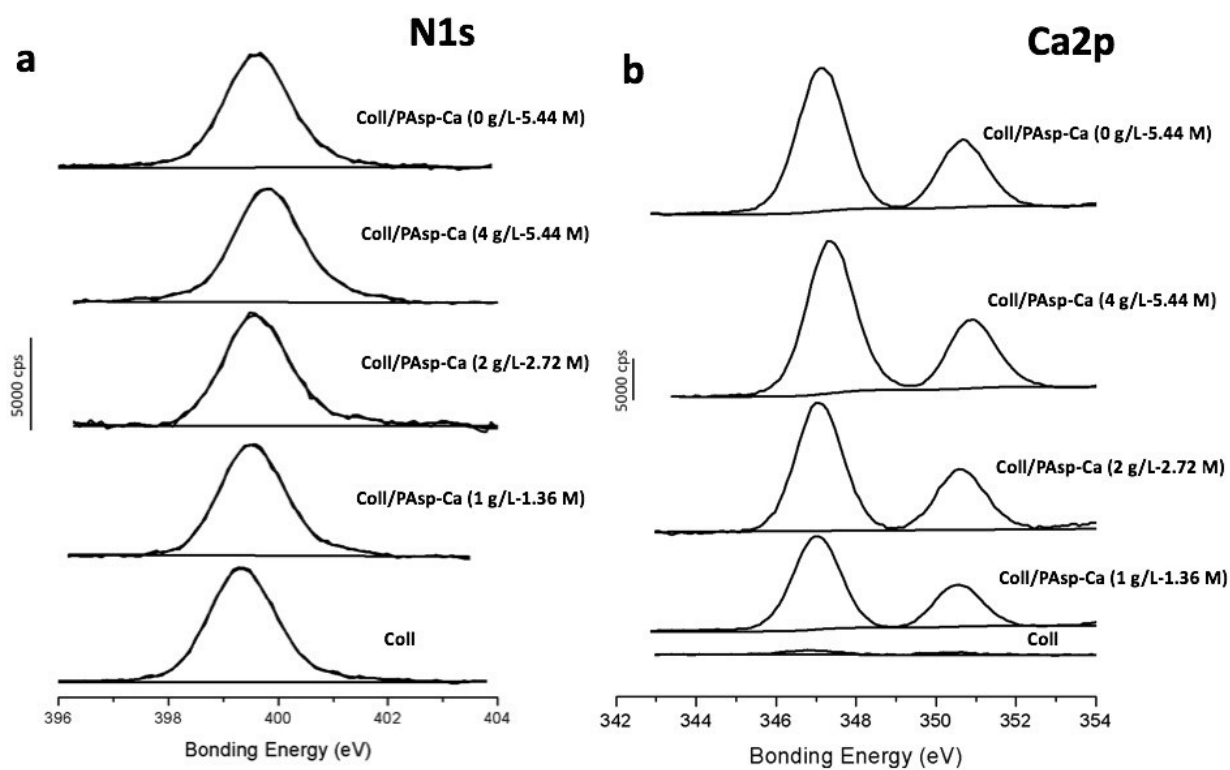


Figure S14. XPS spectra for quantification of the calcium in collagen sponges only treated with a concentration gradient of PAsp-Ca suspensions. After the intensities of N1s peak of the collagen sponges were normalized (a), the intensities of Ca2p (b) were sorted degressively as follows: Coll/PAsp-Ca (4 g/L-5.44 M), Coll/PAsp-Ca (0 g/L-5.44 M), Coll/PAsp-Ca (2 g/L-2.72 M), Coll/PAsp-Ca (1 g/L-1.36 M) and Coll.

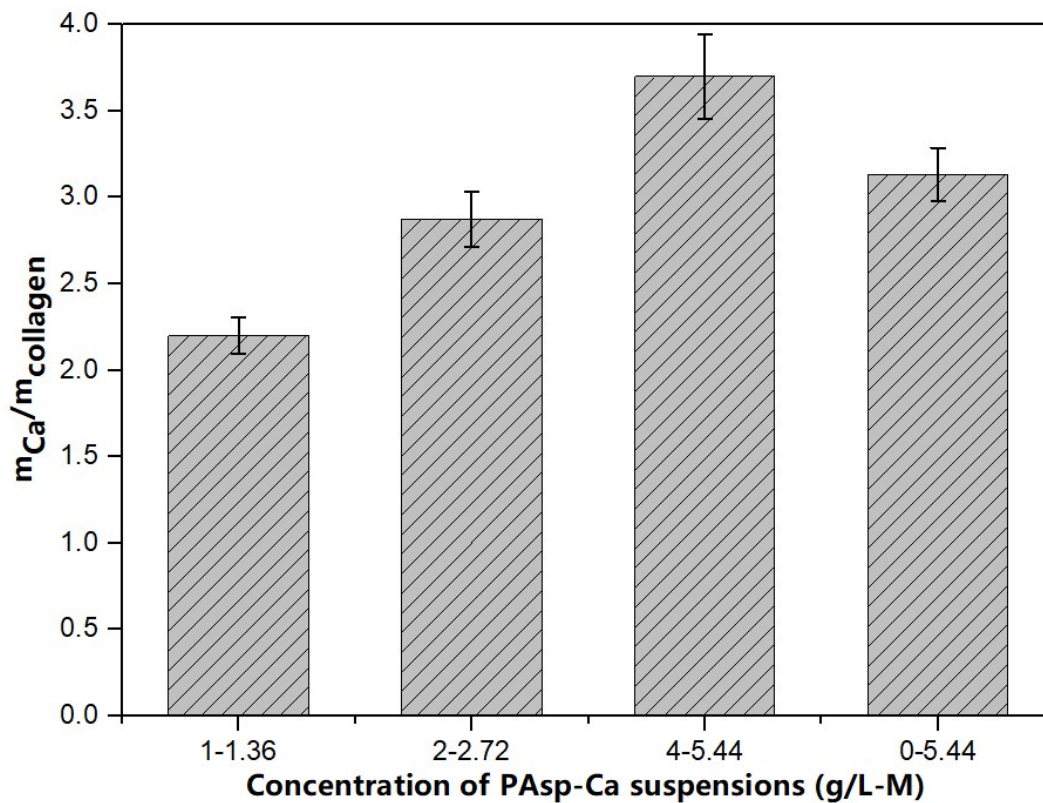


Figure S15. Thermogravimetric analysis for quantification of the calcium content in the collagen sponges only treated with a concentration gradient of PAsp-Ca suspensions. After the collagen sponges were treated with a concentration gradient of PAsp-Ca suspensions (1 g/L-1.36 M, 2 g/L-2.72 M, 4 g/L-5.44 M, 0 g/L-5.44 M), their weight loss of the collagen sponges treated with different suspensions was each measured from 25°C to 600 °C in triplicate. Weight rates of calcium content to collagen were sorted incrementally as follows: 1 g/L-1.36 M, 2 g/L-2.72 M, 0 g/L-5.44 M, 4 g/L-5.44 M.

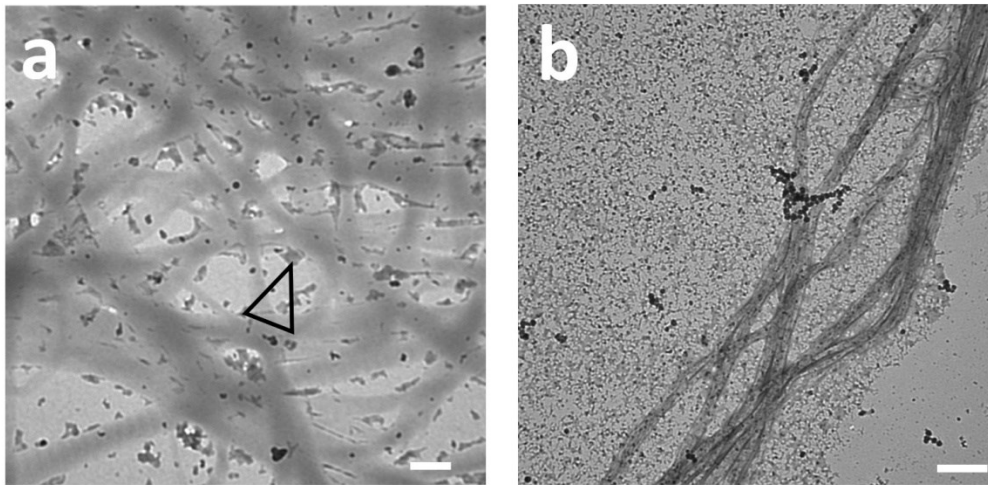


Figure S16. TEM images of the collagen fibrils treated with the PAsp solution, calcium suspension and phosphate solution in sequence. (a) TEM image of the collagen fibrils treated with the PAsp solution (4 g/L, pH = 9.5), calcium chloride suspension (5.44 M, pH = 9.5) and phosphate solution (3.25 M) in sequence, each 3 min. Scale bar: 200 nm. The collagen fibrils are filled with few minerals and ACP is kept outside collagen (open arrowhead). (b) TEM image of the collagen fibrils that are further incubated in the artificial saliva for 1 h, showing poor intrafibrillar mineral. Scale bar: 500 nm.

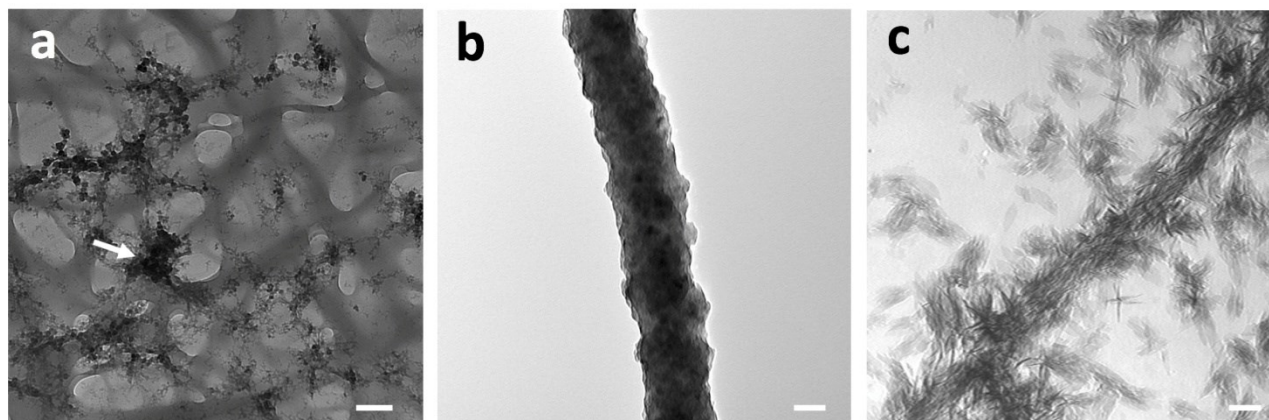


Figure S17. TEM of the collagen fibrils treated with the PAA-Ca suspension (8 g/L-5.44 M) and phosphate solution (3.25 M). (a) The collagen fibrils were treated with the PAA-Ca suspension for 3 min. Scale bar: 200 nm. PAA-Ca complexes (arrow) were attracted onto the collagen fibrils. (b-c) The collagen fibrils were treated with the PAA-Ca suspension and phosphate solution, each 3 min, revealing high electron density of collagen fibrils (b, scale bar: 50 nm), and further incubated in the artificial saliva for 1 h (c, scale bar: 200 nm), revealing heavy extra- and intra-fibrillar mineralization.

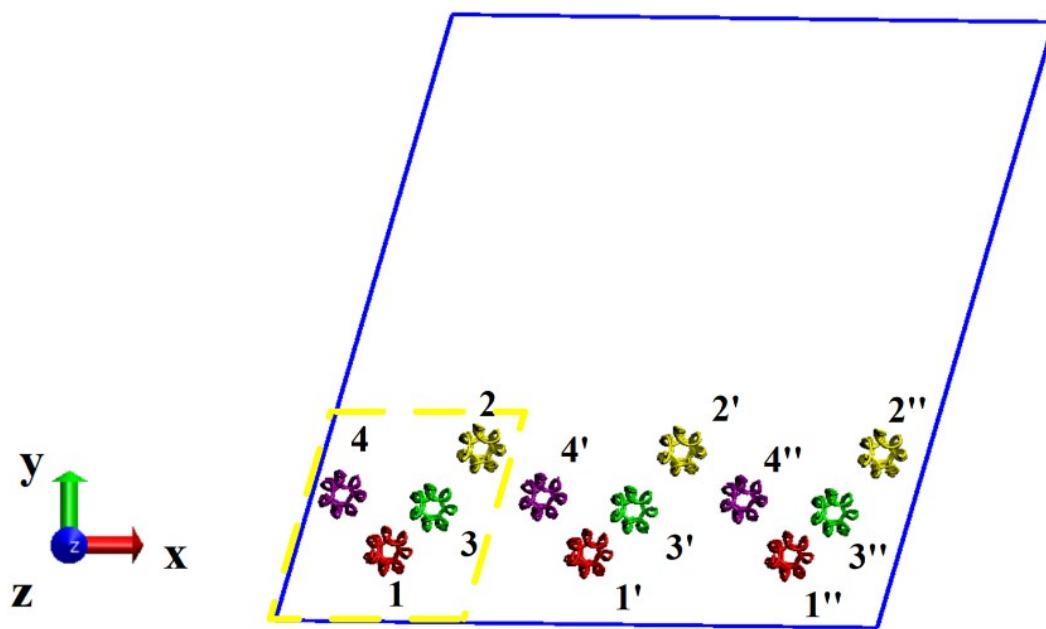


Figure S19. The initial structure of collagen in molecular dynamics simulations. Each unit cell (yellow dotted line) contains four segments of the collagen molecules in the gap zone.

References

- (1) L. Wang, X. An, Z. Xin, L. Zhao and Q. Hu, *J. Food Sci.*, 2007, **72**, 450-455.
- (2) Zhang, Z. H. Huang, S. S. Liao and F. Z. Cui, *J. Am. Ceram. Soc.*, 2003, **86**, 1052-1054.
- (3) J. H. Tao, *Methods Enzymol.*, 2013, **532**, 533-556.
- (4) G. R. Sauer and R. E. Wuthier, *J. Biol. Chem.*, 1988, **263**, 13718–13724.
- (5) S. J. Gadaleta, E. P. Paschalis, F. Betts, R. Mendelsohn and A. L. Boskey, *Calcif. Tissue Int.*, 1996, **58**, 9–16.
- (6) I. Rehman and W. Bonfield, *J. Mater. Sci.: Mater. Med.*, 1997, **8**, 1-4.
- (7) J. P. R. O. Orgel, T. C. Irving, A. Miller and T. J. Wess, *Proc. Natl Acad. Sci. USA*, 2006, **103**, 9001-9005.